The investigation of CO_2 effect on the characteristics of a methane diffusion flame

Halleh Mortazavi, Yiran Wang, Zhen Ma, Yang Zhang[1]

Department of Mechanical Engineering, University of Sheffield, Sir Frederick Mappin Building, Mappin Street, Sheffield, S1 3JD, UK

Abstract

Image processing is used to investigate the effect of mixing carbon dioxide with methane on flame properties by digitally analysing the flame chemiluminescence emission. The images are captured by a high speed colour camera, which is able to record and monitor the spatial and temporal changes in flame chemiluminescence when adding different amounts of carbon dioxide to methane from the moment of ignition to any specific time during combustion. Results confirmed that by increasing carbon dioxide, the flame temperature and soot level are reduced and the flame height is getting longer. On the other hand it has been qualitatively observed that the ignition time is increased. Also, the presence of soot that only emits infrared light is observed during the ignition period. The average value of B/G ratio is calculated through digital image processing. It is found that B/G ratio increases by adding more CO_2.

Keywords: Soot, CO_2, Biogas, Chemiluminescence, Digital image processing, High speed imaging

1. INTRODUCTION

Many researchers showed their interest on the effects of CO_2 addition to hydrocarbon fuels on soot production. This is mainly because of different reasons. One is that CO_2 is one of the main greenhouse gases responsible for

[1]E-mail: yz100@sheffield.ac.uk

global warming which is generally produced due to fossil fuel combustion [1, 2]. One solution to reduce the amount of carbon dioxide is to find alternative environmental friendly fuels. Biogas and bio-syngas are two alternative fuels that recently are in centre of attention [2]. Biogas is produced by fermentation of biomass by anaerobic bacteria and is mainly composed of CH_4 and CO_2[3], whereas Bio syngas is a synthetic gas produced from the thermal gasification of biomass and composed from different proportions of CH_4, H_2, CO and CO_2 [4]. As it can be seen, for both gases, CH_4 and CO_2 are two common components. Note as these gases are produced from different sources, the amount of CO_2 varies from one source to the other source. This causes an impact on the combustion, especially flame stability and soot formation. The soot fraction will also have an impact on the radiation heat transfer characteristics. To have a better design for non-fossil fuel combustion system, well understanding of the influence of mixing CO_2 with CH_4 is a good step forward. Many valuable contributions have been done in this area [5, 6, 7] and it is known that adding CO_2 causes soot suppression in the combustion process [8]. Yet, it is not precisely known under which procedure the soot level reduces [9]. It is found that soot formation is affected by three classes of operation, diluent, thermal and chemical [10, 11]. The dilution effect is due to reduction of the species, and therefore reducing their collision frequencies. The thermal effect is due to the change in flame temperature. The chemical effect is due to the participation of additives in reactions related to soot formation. Considering that these three effects are not acting independently, and they do have effect on the performance of each other. Different soot measurement techniques are proposed and improved by scientists, which can be categorised into two main approaches, invasive and non-invasive techniques [12]. In invasive techniques direct sampling is taken from the combustion area. Molecular beam mass spectrometry (MBSM) is an example of invasive technique, where a probe is inserted in the flame area very fast to take the sample [13]. Although it takes direct information, but during sampling a strong perturbation occurs, which results in a change to the chemical reactions in combustion area [14]. Non-invasive methods take advantage of flame

optical properties. Despite the fact that some non-invasive techniques might be complicated or costly, the advantage is the combustion area is not touched, and also a spatial and temporal information can be collected. Various number of non-invasive approaches are established and developed by researchers for different applications. Popular examples are Laser-induced incandescence (LII) [15, 16], multiwavelength [17], chemiluminescence based [2] and digital imaging techniques [18, 19]. Colour is one of the inherent specifications of flame. The sensation of colour by human eye is generally due to receive the emitted or reflected light in a specific range of light spectrum, 400-720nm. Colour can be specified and created by colour spaces. Several colour spaces are proposed such as CIE, RGB, sRGB, HSV, HSI for different applications [20]. In this work, RGB and HSV colour spaces are employed. RGB is the common colour space which is often found in computer systems and camera devices. In RGB, colours are specified in terms of three primary colours red (R), green (G) and blue (B), which can be displayed as a cube. Although the RGB colour space provides a straightforward way to display colour images, but it is not always the best choice for processing and analysis. One of the disadvantages is the inability to separate the colour information from the intensity. HSV colour space represents colour in terms of Hue (colour depth), Saturation (colour purity) and Value (Colour brightness). Hue refers to colour type, such as red, blue or yellow. It takes values from 0^o to 360^o. Saturation refers to the purity of the colour. It takes values from 0-100%. The lower saturation of a colour, the more faded the colour is represented. Finally, Value component refers to the brightness of the colour. It takes the same range as saturations, 0-100%. The appearance of flame colour depends on several conditions during combustion process, such as burning condition, fuel composition and equivalence ratio (ϕ) [21]. Flame colour is mostly because of the chemiluminesence emission in visible light spectrum of radicals and soot particles produced during the chemical reactions of combustion process. Chemiluminesence is in fact the emitted light due to the de-excitation of excited radicals during the chemical process of combustion [22]. It is found in previous studies that CH* intensity radiation peak at 431nm, and C_2* intensity

radiation peak at 516nm, are responsible for the variable degree of blue-green flame colour (asterisk (*) denotes the electronically excited state species) [21]. While the soot particles are responsible for yellow-orange colour in flame [21]. Considering that some species and radicals chemiluminesence emission are out of visible range and cannot be seen by eye, such as OH* radical, intensity radiation peak at 309nm [2], or some soot particles appear at early stage of ignition, which are in infrared region [21]. These known spectral signatures can be used to extract and provide hidden flame information in combustion zone. Recently, many combustion applications, such as monitoring, modelling and diagnosing the combustion system, have used flame chemiluminesence emission [23, 24]. Human eye is not only limited in sensing the radiation intensity in small scale of light spectrum, but also it is limited in detecting fast moving objects and can only sense moving objects equivalent to a camera standard speed up to 25fps. The chemical reactions and turbulence in combustion are taking place very fast, and human eye is not able to detect the flame dynamics. Recent studies showed that it is feasible to capture combustion process by using high speed camera (3000fps) with acceptable resolution (1024×1024) [18]. Also, it is shown that some cameras can detect the emissions in some parts of infrared spectral regions [21]. Hunag & Zhang [21, 18] proposed a non-invasive technique, Digital Flame Colour Discrimination (DFCD), to investigate flame characteristics by applying digital image processing to digital colour flame images which are captured by a high speed camera. Within DFCD it is possible to track the spatial and temporal prescence of soot as well as the chemiluminescence emissions of CH* and C_2* in visible range. Also, invisible soot during ignition time, which is in infrared can be tracked. Details of DFCD technique on processing and analysing flame images are well explained and available in [21, 18, 19]. The main goal of this study is to employ DFCD technique to investigate the effects of mixing CO_2 with methane gas on soot production and the presence of CH* and C_2* in combustion area. The effects on flame height and temperature are also examined. Recent developed version of colour band two-colour method [25, 26], is employed here to measure flame temperture. In two-colour method, flame

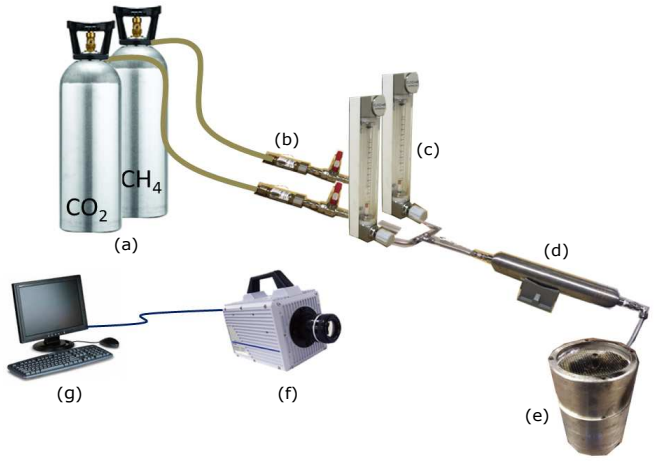

Figure 1: The schematic of experimental setup a) Gas cylinders, b) Connecting pipes, c) Rotameters, d) Mixing gas cylinder, e) Bunsen burner, f) High speed camera, g) Computer with Photron software.

images are captured in RGB colour format. Any two combinations of these three red (R), green (G) and Blue (B) colour channels can be used for flame temperature determination. In order to avoid image saturation caused by the very intense soot light emission, the high speed camera is set to a high shutter speed ($\frac{1}{10000}$s).

2. EXPERIMENTAL SETUP & PROCEDURE

The experimental setup is consisted of the high speed colour camera, fuel gas cylinder, rotameters for flow measurement, gas mixing cylinder and Bunsen burner. The schematic of the experimental setup is shown in Figure1.

Fuel gases, CH_4 and CO_2, are supplied from gas cylinders. Each cylinder is connected by pipe, with 6mm diameter, to a separate mechanical rotameters. A gas mixing chamber with 500cm^3 capacity is used to mix the gases well before reaching the burner. The input of the mixing cylinder is from a gas line coming from the flow meters, and the output is connected by pipe to the Bunsen burner, with outer nozzle diameter 8.94mm and honeycomb mesh. The

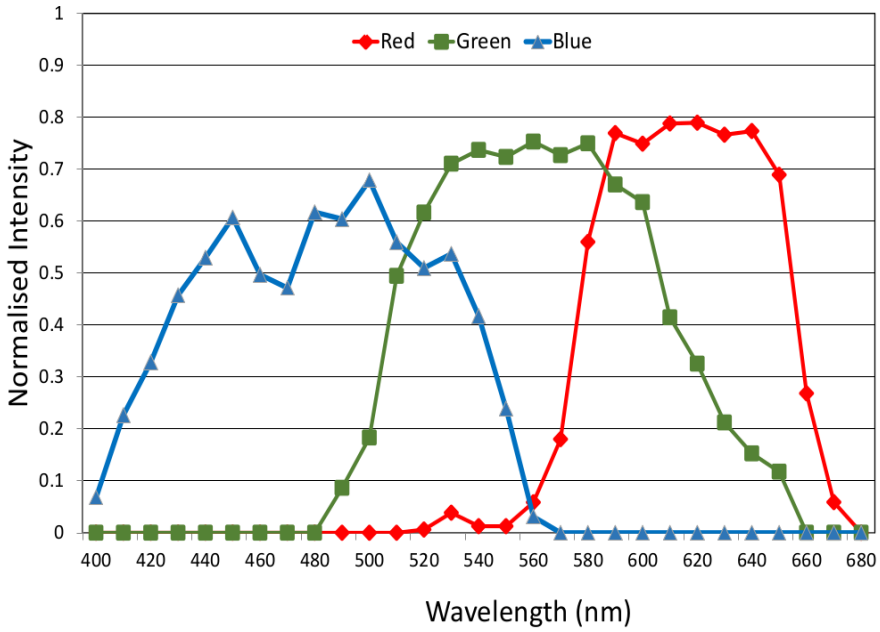

Figure 2: Photros Fastcam SA4 camera spectral response.

ignition is activated by an electrode device with approximately 30kV output voltage. Pair of steel electrodes is kept apart, 9mm, from each other. High speed CMOS camera 'Photron Fastcam SA4' is used to capture images with 1024×1024 pixel resolution. The spectral response of the camera is investigated in previous research [27] and is given in Figure 2. The high speed camera frame rate and shutter speed are set to 500fps and $\frac{1}{800}$s respectively for soot study. The camera is connected to a computer having $PHOTRON$ software for setting the camera parameters, and also capturing and saving images in RGB (Red-Green-Blue) colour space. The post processing and analysing of flame images are done on Matlab routine, which is written in previous study [21], where captured flame images are converted to HSV (Hue-Saturation-Value) colour space. The presence of CH* & C2* and soot can be easily distinguished, as the colour of CH* & C_2* appears in 180^o-300^o and soot appears in 1^o-80^o of Hue channel.

Eight sets of experiment are conducted with different mixing rate of methane

Table 1: Different amount of added CO_2 with methane, and corresponding velocity and Reynolds No.

Case	1	2	3	4	5	6	7	8
CO_2 (l/min)	0	0.123	0.37	0.618	1.236	1.854	2.47	3.09
CO_2%	0	12	37	61	123	185	247	309
CH_4 (l/min)	1	1	1	1	1	1	1	1
Velocity (m/min)	0.159	0.179	0.218	0.258	0.356	0.455	0.553	0.652
Re No	0.0086	0.0108	0.0152	0.0196	0.0306	0.0416	0.0525	0.0636

and CO_2. Methane flow rate is set to 1l/min for all cases and carbon dioxide flow rate is varied as shown in Table 1. Camera settings, the position of the camera and burner are fixed and kept unchanged throughout the whole experiment.

To measure the flame temperature, SiC fibre with $15\mu m$ thickness is placed in a frame, located at top of the Bunsen burner, in a way to cover different areas of flame. The fibres are 1.5cm apart. SiC fibres involving in the measurement plays a role of greybody radiation emitters, as the flame becomes soot deficient. The camera for temperature measurement is set to frame rate 1000fps and shutter speed $\frac{1}{10,000}$s. The very high shutter speed is necessary to avoid image saturation. The analysis of flame temperature from digital images is based on two-colour method that has been widely used over last decade [28]. The detectable temperature range within this measurement method is between 1300K-2400K [29]. The accuracy of two-colour measurement is verified by measuring the temperature of the tungsten lamp within the error of 3 percent and comparing with infra-pyrometer on measuring fiber temperature [29]. Detail of the methodology is available in[26].

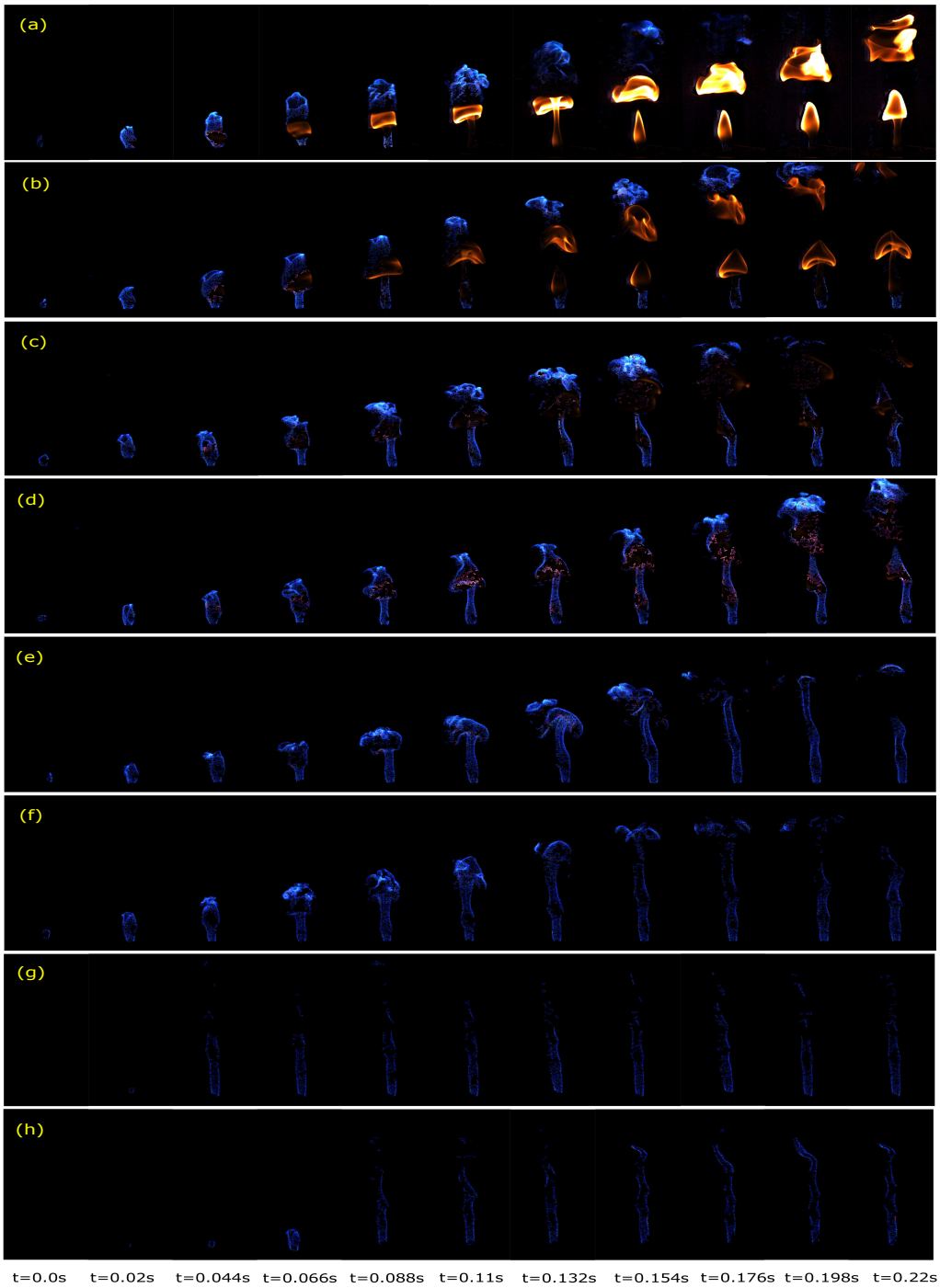

Figure 3: Sample flame images of mixing methane with different levels of CO_2, a) Case1, b) Case2, c) Case3, d) Case4, e) Case5, f) Case6, g) Case7, h) Case8.

3. RESULTS

The sample of captured flame images at t=0sec - 0.22sec for different cases are presented in Figure 3. The intensity of blue pixels in cases 2-8 are enhanced by magnifying 50 times (50 out of 255) in order to be presented. It can be seen that the flame colour has dramatically changed from bright yellow-orange to orange-blue colour as soon as CO_2 is introduced. From Case3 afterwards, by increasing the level of CO_2, the yellow-orange colour is gradually faded and disappeared and flame only appears in blue colour. Note that for Case1, CO_2 = 0% , some pixels in flame images seems to be saturated. This is unavoidable. At first, diffusion methane, the flame colour is bright (yellow-orange) light. For other cases the dominant flame signal become blue, which is a weak signal and hard to be captured by the camera sensor. Therefore, the camera should be set in a way to be able to capture weak blue signals in later cases and as we want to have a fair comparison between different flame images. The camera position and setting are unchanged throughout the experiment.

It has been observed that as the level of CO_2 increased the ignition time delayed more. Case8, CO_2 = 309%, is the maximum limit of adding CO_2 to methane because it was very difficult to ignite the flame, and also, after ignition the flame will easily blow out. This shows the limit for maximum amount of CO_2 that can be added.

3.1. Flame colour

3.1.1. Soot flame (Orange) region

Orange region refers to hue channel space of 0^o-40^o from HSV colour image format, which represent the soot broadband emissions. Figure 4(a) shows the 3D plot of temporal variation of the number of pixels in orange region. It can be seen that the number of orange pixels at Case1, has the highest level. By introducing CO_2 at Case2 the orange pixels drop and at Case4, the number of orange pixels is close to zero, and hardly can be seen. After Case4 no orange pixel exists. This implies the soot level is very high for pure methane diffusion

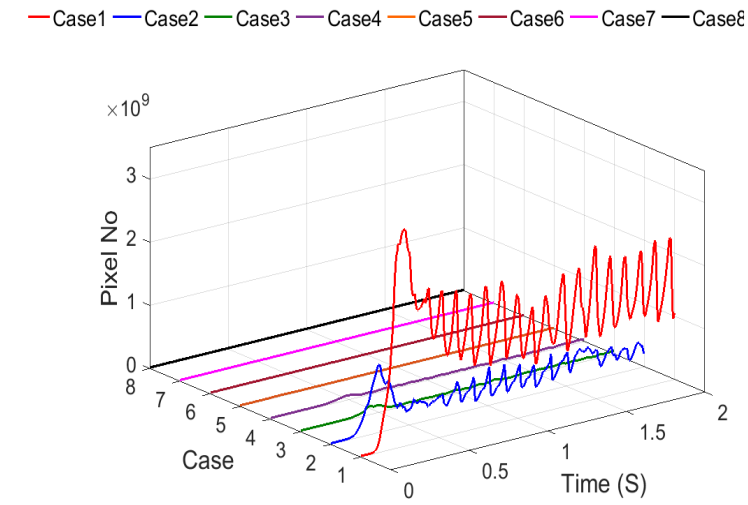

(a) Orange

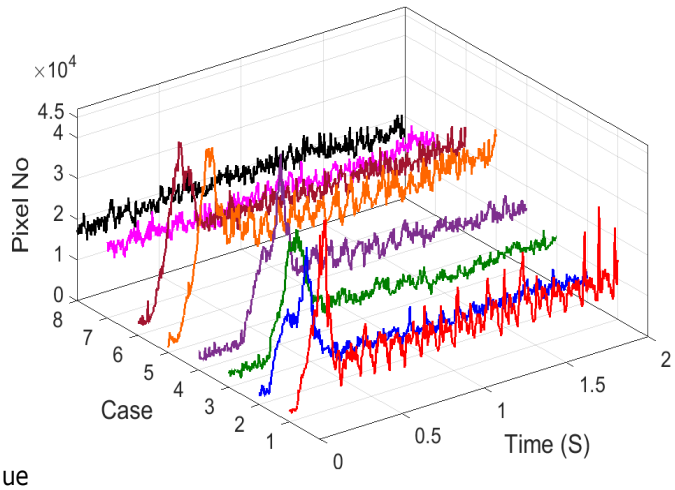

(b) Blue

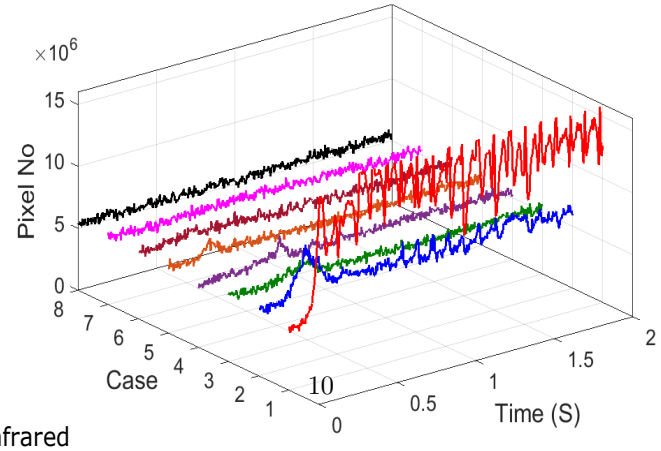

(c) Infrared

Figure 4: The plot of number of pixels in continuous flame images of 2s in duration a) Orange region, b) Blue region c) Infrared region for all the 8 cases.

flame (Case1) and mixing CO_2 with methane causes reduction in soot level. When the volume flow rate of CO_2 is half the methane, no soot is detectable.

3.1.2. Blue flame region

Blue flame region refers to hue channel space of 130^o-252^o from HSV colour image format, which represents CH* and C_2*. Figure 4(b) shows the 3D plot of temporal variation of the number of pixels in blue region. It can be seen that the number of blue pixels at Case1, is at lowest level. Only at early ignition time, some blue pixels can be detected, and when flame gets stable, blue pixels are nearly zero. By the time CO_2 is added, from Case2 afterwards, the number of blue pixels gradually increased and they reached to maximum level at Case4. From Case4 to 8 the number of blue pixels remains nearly the same. This implies that the area of CH* and C_2* radicals increased due to added CO_2. A sharp peak can be seen at the begining of the plots of the first cases. This is because of the excess of the fuel in the pipe at ignition time.

3.1.3. Infrared region

The recent research has shown that the colour camera is able to detect some infrared emission and it is found that the infrared colour corresponds to hue channel space of $252^o - 360^o$ from HSV colour image format, which represents soot particles appear at early stage of the ignition process.

Figure 4(c) shows the 3D plot of temporal variation of the number of pixels in infrared region. It can be seen that the number of infrared pixels has the highest amount at t<0.4sec for Cases1-4. At Case5, the infrared pixels decrease dramatically even during the ignition period. From Case6 afterwards, no infrared pixels is detected even in early ignition period.

3.2. Flame temperature

It is shown in previous study that the Sic fibre temperature is proportional to the flame temperature[30]. Therefore, the trend of temperature variation by adding CO_2 is examined by measuring the temperature of the fibres in this experiment. Figure 5 shows a sample of flame image with fibres installed for

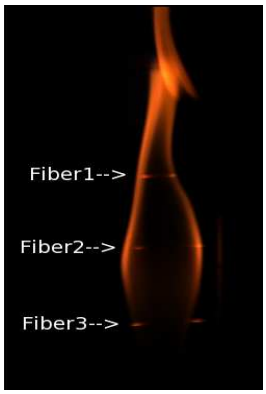

Figure 5: Sample of flame image at temperature experiment.

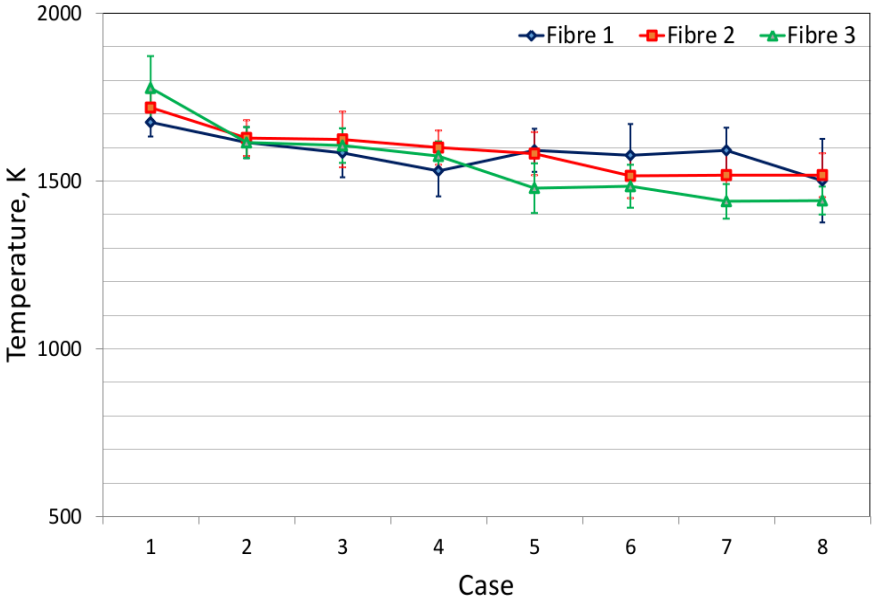

Figure 6: The plot of mean fibre temperature of 1000 continuous images with respect to different levels of added CO_2 with relative value of standard deviation.

temperature measurement. The mean temperature and correspnding standard deviation of 1000 continuous images (1sec) at each fibre and for all the 8 cases are calculated and presented in Figure6. It can be seen, as soon as adding

CO_2 to diffusion methane, the flame temperature at 3 different fibre locations has dropped. Comparing the plots of Figure6 indicates that the temperature variation at fibre 2 and 3 show good agreement. However, fibre 1 which is more away from the nozzle and close to the flame tip, shows some instability after Case4. This may be mainly correlated with the buoyancy-driven oscillation that is associated with the Kelvin-Helmholtz instability and the considerable number of vortices appearing due to the buoyant interaction between the cold ambient air and the hot burnt gases. Shepherd [31] used a joint experimental and numerical approach to demonstrate the formation of the vortices near the flame tip, and to explain how flame flicker occurs from heat release at the flame front, which compels the burnt gas flow in a radial direction opposed to the rotating vortex motion induced in the pressure field. This explains the increase of the flame temperature instability from the flame base to the tip.

3.3. Flame height

Fifteen flame sample flame images are selected from t=1.5 secs of captured images with time intervals of 0.1 seconds. The average of flame heights for different levels of added CO_2 are found in pixel space in vertical dimension (image length). Each pixel approximately corresponds to 0.2mm. Figure 7 presents the plot of flame height versus different amounts of added CO_2. It can be seen at the beginning, where soot presents in flame, mixing CO_2 decreases the flame height. Then after, when the soot is faded after Case3, and the flame colour turns to pure blue, flame height increases by adding more CO_2. The increment of flame height is because of the change in reaction rate. As the flow rate is constant, by decreasing the reaction rate the flame area increases. As it is seen in flame temperature chart, the temperature decreases which means decreasing the flame reaction rate. The reason for the flame height decrement at first two cases is not known and further investigation is required.

3.4. B/G Ratio

It is shown in previous study [18] that the value of each pixel in blue channel (RGB colour space) with respect to the value in green channel, B/G ratio,

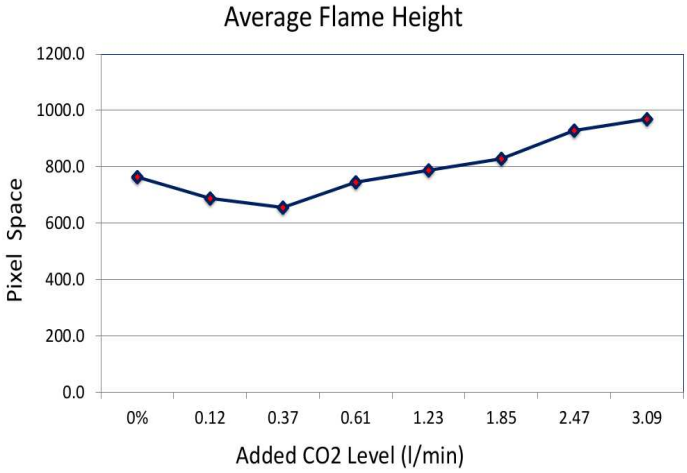

Figure 7: The plot of flame height (in pixels) versus different percentage of mixing CO_2.

corresponds to the presence of CH*/C_2* in the flame spatial position. The B/G ratio is calculated for each pixel position in flame images for all cases of added CO_2. The mean value of each image with value higher than zero can be calculated to see the variations. Figure 8 presents the 3D plot of the mean B/G ratio for 2s of flame image duration for all the 8 cases. It is shown that the average B/G ratio increases by adding more CO_2, which means the average increasing rate of CH* radicals are more than that of C_2* radicals. The underlying physics needs further investigation.

4. CONCLUSION

Digital image processing is applied to investigate the effect of mixing CO_2 to methane gas. The results have shown that by increasing CO_2, the level of soot emissions in visible spectrum reduces. No soot is detectable if the volume flow rate of CO_2 reaches around half of the CH_4 volume flow rate. Also, the amount of CH* and C_2* radicals increased by increasing CO_2, and it reaches to maximum when CO_2 flow rate reaches around half of the amount of CH_4 flow rate. The B/G ratio, which corresponds to CH*/C_2*, increases by increasing CO_2. Moreover, the amount of pixels for infrared soot particles are detectable

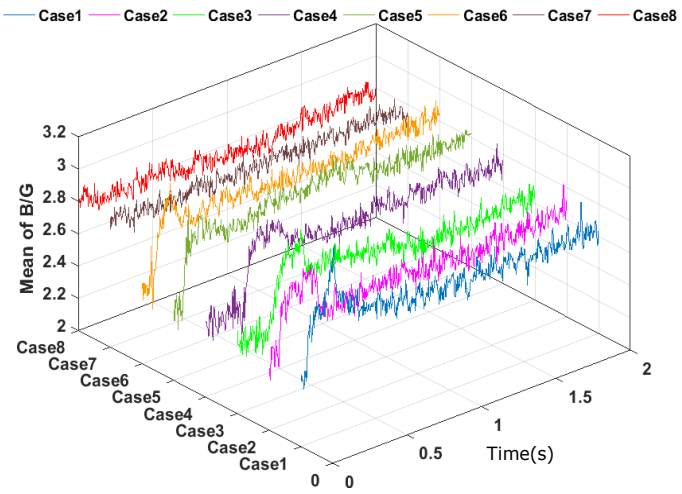

Figure 8: The plot of B/G ratio (mean value) in continuous flame images of 2s in duration for all the 8 cases.

and nearly have the same amount till Case5 and afterwards, hardly any infrared pixels can be detected. This might be related to the fact that considerable ignition delay has been observed during the experiment when the CO_2 flow rate is greater than the CH_4 flow rate (Case6 afterwards).

In this work, it is shown the capability of image processing in flame temperature meaurement. In previous studies, it was found that flame temperature decreases by adding CO_2, and in this work the same result was shown by digital image processing technique.

It has been shown that the flame height increases by increasing CO_2 after CO_2 flow rate is higher than half of the CH_4 flow rate. When CO_2 flow rate is lower than CH_4 flow rate (soot is detectable at this stage), flame height decreases. The reason is not exactly clear, and further investigation is required.

Acknowledgement

This work is funded by EPSRC through the grant no EP/K036750/1.

References

[1] D. Hainsworth, M. Pourkashanian, A. P. Richardson, J. L. Rupp, A. Williams, The influence of carbon dioxide on smoke formation and stability in methane-oxygen-carbon dioxide flames, Fuel 75 (3) (1996) 393–396.

[2] T. Garcia-Armingol, J. Ballester, Influence of fuel composition on chemiluminescence emission in premixed flames of CH4/CO2/H2/CO blends, International Journal of Hydrogen Energy 39 (35) (2014) 20255–20265.

[3] M. Fischer, X. Jiang, An investigation of the chemical kinetics of biogas combustion, Fuel 150 (2015) 711–720.

[4] M. Fischer, X. Jiang, An assessment of chemical kinetics for bio-syngas combustion, Fuel 137 (2014) 293–305.

[5] A. R. A. Aziz, A. B. Wasiu, M. R. Heikal, The effect of carbon dioxide content-natural gas on the performance characteristics of engines: A review, Journal of Applied Sciences 12 (23) (2012) 2346–2350.

[6] P. Glarborg, L. L. Bentzen, Chemical effects of a high CO2 concentrations in oxy-fuel combustion of methane, Energy & Fuels 22 (1) (2008) 291–296.

[7] K. C. Oh, H. D. Shin, The effect of oxygen and carbon dioxide concentration on soot formation in non-premixed flames, Fuel 85 (5-6) (2006) 615–624.

[8] F. Liu, H. Guo, G. J. Smallwood, O. L. Gulder, The chemical effects of carbon dioxide as an additive in an ethylene diffusion flame implications for soot and nox formation, Combustion and Flame 125 (2001) 778–787.

[9] D. X. Du, R. Axelbaum, C. Law, The influence of carbon dioxide and oxygen as additives on soot formation in diffusion flames, Symposium (International) on Combustion 23 (1) (1991) 1501–1507.

[10] J. Park, D. Hwang, J. Chio, K. Lee, S. Keel, S. Shim, Chemical effects of CO2 addition to oxidizer and fuel streams on flame structure in H2-

O2 counterflow diffusion flames, Int. Journal of Energy Research 27 (2003) 1205–1220.

[11] M. R. Charest, O. L. Gulder, C. P. Groth, Numerical and experimental study of soot formation in laminar diffusion flames burning simulated biogas fuels at elevated pressures, Combustion and Flame 161 (2014) 2678–2691.

[12] C. S. McEnally, A. M. Schaffer, M. B. Long, L. D. Pfefferle, M. D. Smooke, M. B. Colket, R. J. Hall, Computational and experimental study of soot formation in a coflow, laminar ethylene diffusion flame, Symposium (International) on Combustion 27 (1) (1998) 1497–1505.

[13] N. Hansen, T. A. Cool, P. R. Westmoreland, K. Kohse-Hoinghaus, Recent contributions of flame-sampling molecular-beam mass spectrometry to a fundamental understanding of combustion chemistry, Progress in Energy and Combustion Science 35 (2) (2009) 168–191.

[14] A. Hartlieb, B. Atakan, K. Kohse-Hoinghaus, Effects of sampling quartz nozzle on the flame structure of a fuel-rich low-pressure propane flame, Combustion and Flame 21 (4) (2001) 610–624.

[15] B. Quay, T. W. Lee, T. Ni, R. J. Santoro, Spatially resolved measurements of soot volume fraction using laser-induced incandescence, Combustion and Flame 97 (3-4) (1994) 384–392.

[16] K. C. Oh, H. D. Shin, The effect of oxygen and carbon dioxide concentration on soot formation in non-premixed flames, Fuel 85 (2006) 615–624.

[17] S. D. Iuliis, M. Barbini, F. Cignoli, G. Zizak, Determination of the soot volume fraction in an ethylene diffusion flame by multiwavelength analysis of soot radiation, Combustion and Flame 115 (1-2) (1998) 253–261.

[18] H. W. Huang, Y. Zhang, Dynamic application of digital image and colour processing in characterizing flame radiation features, Measurement Science and Technology 21 (8).

[19] H. W. Huang, Y. Zhang, Digital colour image processing based measurement of premixed CH4 + air and C2H4 + air flame chemiluminescence, Fuel 90 (1) (2011) 48–53.

[20] M. D. Fairchild, Color Appearance Models, 3rd Edition, Wiley, 2013.

[21] H. W. Huang, Y. Zhang, Flame colour characterization in the visible and infrared spectrum using a digital camera and image processing, Measurement Science and Technology 19.

[22] J. Kojima, Y. Ikeda, T. Nakajima, Spatially resolved measurement of OH* , CH*, and C2* chemiluminescence in the reaction zone of laminar methane/air premixed flames, Proceedings of the Combustion Institute 28 (2000) 1757–1764.

[23] D. Sun, G. Lu, H. Zhou, Y. Yan, Flame stability monitoring and characterization through digital imaging and spectral analysis, Measurement Science and Technology 22 (11).

[24] T. Garca-Armingol, J. Ballester, Flame chemiluminescence in premixed combustion of hydrogen-enriched fuels, International Journal of Hydrogen Energy 39 (21) (2014) 11299–11307.

[25] H. Zhao, N. Ladommatos, Oprical diagnostics for soot and temperature measurement in diesel engines, Progress in Energy and Combustion Science 24 (3) (1998) 221–255.

[26] Z. Ma, Y. Zhang, High temperature measurement using very high shutter speed to avoid image saturation, AIP Conf Proceeding 1592 (1) (2014) 246–253.

[27] J. Yang, Z. Ma, Y. Zhang, A novel flame chemiluminescence measurement using a digital colour camera, 25th ICDERS, Leeds, UK (2015) 1–6.

[28] Y. Huang, Y. Yan, Transient two-dimensional temperature measurement of open flames by dual-spectral image analysis, Transactions of the Institute of Measurement and Control 22 (5) (2000) 371–384.

[29] Z. Ma, Two-colour temperature measurement based on high speed imaging, Ph.D. thesis, The School of Mechanical Engineering, University of Sheffield (Dec. 2016).

[30] B. Ma, G. Wang, G. Magnotti, R. S. Barlow, M. B. Long, Intensity-ratio and color-ratio thin-filament pyrometry uncertainties and accuracy, Combustion and Flame 161 (4) (2014) 908–916.

[31] I. Shepherd, R. Cheng, M. Day, The dynamics of flame flicker in conical premixed flames an experimental and numerical study, eScholarship, University of California.